Plasma-catalytic reforming of CO_2-rich biogas over Ni/γ-Al_2O_3 catalysts in a rotating gliding arc reactor

Fengsen Zhu[a,c], Hao Zhang[b], Xin Yan[a], Jianhua Yan[a], Mingjiang Ni[a], Xiaodong Li[a,*], Xin Tu[c,*]

[a] State Key Laboratory of Clean Energy Utilization, Zhejiang University, Hangzhou 310027, China

[b] Institute of Energy and Power Engineering, College of Mechanical Engineering, Zhejiang University of Technology, Hangzhou 310014, China

[c] Department of Electrical Engineering and Electronics, University of Liverpool, Liverpool L69 3GJ, UK

***Corresponding authors**

Dr. Xin Tu

Department of Electrical Engineering and Electronics,

University of Liverpool,

Liverpool, L69 3GJ,

UK

E-mail: xin.tu@liverpool.ac.uk

Prof. Xiaodong Li

State Key Laboratory of Clean Energy Utilization,

Zhejiang University,

Hangzhou 310027,

China

E-mail: lixd@zju.edu.cn

Abstract

The combination of plasma and heterogeneous catalysis has been considered as an attractive and promising process for the synthesis of fuels and chemicals. In this work, plasma-catalytic reforming of biogas is carried out over Ni/γ-Al_2O_3 catalysts with different Ni loadings (6 wt.%, 8 wt.% and 10 wt.% Ni) in a novel rotating gliding arc (RGA) plasma reactor. In the plasma reforming of biogas without a catalyst, the CH_4 conversion can reach up to 52.6% at a CH_4/CO_2 molar ratio of 3:7 and a total flow rate of 6 L/min. The combination of the RGA with the Ni/γ-Al_2O_3 catalysts enhances the performance of the plasma biogas reforming: increasing Ni loading enhances the conversion of CH_4 and the maximum CH_4 conversion of 58.5% is achieved when placing the 10 wt.% Ni/γ-Al_2O_3 catalyst in the downstream of the RGA reactor. The presence of the 10 wt.% Ni/γ-Al_2O_3 catalyst in the RGA reactor also increases the H_2 yield by 17.6% compared to the reaction in the absence of a catalyst. A comparison of biogas reforming using different plasma technologies shows that the RGA plasma provides a higher conversion, significantly enhanced processing capacity and reduced energy cost for biogas conversion and syngas production. In addition, compared to biogas reforming using other non-thermal plasmas (e.g. dielectric barrier discharge), the RGA reforming process produces much cleaner gas products in which syngas is the major one.

Keywords: Rotating gliding arc (RGA); Plasma-catalysis; Biogas reforming; Syngas

1. Introduction

Biogas generated from wastewater treatment, anaerobic digestion of biomass, and landfills has been regarded as a promising renewable energy source to respond to the global energy and environmental challenges. Biogas mainly consists of combustible CH_4 and non-combustible CO_2, and can be used for generating heat and power. However, due to the presence of CO_2, low calorific value (LCV) of biogas is one of the major barriers of biogas development in the combined heat and power (CHP) generation [1-3]. Different technologies have been developed for the upgrading of biogas to bio-methane, which is an excellent fuel for a large number of applications and can also be used as raw material for the production of chemicals. However, biogas upgrading is an energy and capital intensive process.

Reforming of biogas (also called dry reforming) without prior CO_2 separation is considered as an attractive and sustainable alternative to produce syngas (CO and H_2), which is an important chemical feedstock for the production of a range of platform fuels and chemicals [4]. However, biogas reforming is a thermodynamically unfavorable reaction and high operating temperatures (>700 ^{o}C) are required to obtain reasonable conversions of stable and inert molecules CO_2 and CH_4, which incurs high energy cost of the process. A range of supported metal catalysts (e.g. Ni, Co, Pt, Pd, etc) have been used to lower the activation energy of biogas reforming reaction [5, 6]. Ni based catalysts have been widely used in this reaction considering their activity, availability and cost [7-10]. However, rapid catalyst deactivation due to coke formation and deposition remains a major challenge in the reforming of CH_4 and CO_2, and limit the use of this process on a commercial scale [11,12].

Non-thermal plasmas offer an attractive and relatively unexplored alternative as means for the

synthesis of fuels and chemicals, offering a unique way to enable thermodynamically unfavourable reactions (e.g. biogas reforming) to occur at atmospheric pressure and low temperatures. Non-thermal plasmas show a unique non-equilibrium character and can generate highly energetic electrons and a variety of chemically reactive species including radicals, excited atoms, molecules and ions, which are capable of initiating a variety of physical and chemical reactions, the dominant pathways being determined by plasma processing conditions. Various non-thermal plasmas have been investigated for converting biogas into syngas, including dielectric barrier discharge (DBD) [13-15], corona discharge [16], glow discharge [17], microwave discharge [18] and gliding arc (GA) [12]. However, in the absence of a catalyst, a range of products could be produced in the plasma reforming reaction with lower selectivity towards desirable products (e.g. syngas) compared to that achieved using traditional catalytic process, which limits the use of plasma process in an industrial scale [19].

Recently, hybrid plasma-catalytic process has attracted significant interest for the synthesis of value-added fuels and chemicals due to combined advantages of fast and low temperature reaction by non-thermal plasmas and selective synthesis from catalysis. This novel hybrid process has great potential to generate a synergistic effect, resulting from the physical and chemical interactions between the plasma and catalyst, to enhance the conversion of reactants and the selectivity/yield of the desired products, whilst reducing the energy consumption of the plasma-catalytic process [20-22]. Song et al. [23] reported that the CO selectivity was increased by 23.7% in the plasma biogas reforming over a Ni/γ-Al_2O_3 catalyst in a DBD reactor, compared to the plasma reaction without a catalyst. Similar result was obtained by Long et al. [24] using a plasma-jet reactor. Tu et al. [14] investigated the effect of three different catalyst packing methods on the plasma-catalytic

dry reforming of CH_4 over Ni/Al_2O_3 catalysts in a DBD reactor at ~250 ^oC. They found that partially packing the Ni/Al_2O_3 catalyst with a low calcination temperature (300 ^oC) in the DBD significantly enhanced plasma-catalyst interactions, thus generating a synergistic effect with doubled CH_4 conversion and H_2 yield compared to the plasma reaction without a catalyst under the same conditions. Most of previous works on plasma-catalytic reforming of biogas have been carried out using dielectric barrier discharges as it is easy to integrate catalysts with a DBD reactor. However, the energy efficiency of the plasma reforming process using a DBD even with a catalyst is still significantly lower than those using gliding arc plasmas [25].

In this study, a novel rotating gliding arc (RGA) reactor, co-driven by a tangential gas flow and a magnetic field, has been developed for the conversion of biogas into value-added fuels and chemicals. With the combined effects of swirling flow and Lorentz force, the arc can rotate rapidly and steadily around an inner cone-shaped electrode, providing a stable and large three-dimensional plasma region with enlarged retention time of the reactants, which favours chemical reactions. Our previous works have shown that the use of the RGA plasma can significantly enhance the performance (e.g. conversion and energy efficiency) of plasma chemical reactions for the synthesis of fuels and chemicals, compared to traditional gliding arcs with knife-shaped electrodes or other non-thermal plasmas (e.g. DBD) [26-28]. The combination of the rotating gliding arc with suitable catalysts has great potential to further enhance the energy efficiency of the plasma reforming process and make it more attractive. However, it is a great challenge to integrate catalysts with either flat gliding arc or rotating gliding arc due to a high gas flow. Up until now, very limited work has been dedicated to the combination of gliding arc discharge with catalysts for the synthesis of fuels and chemicals, while the integration of the RGA with a catalyst has not been reported. In this

work, Ni/γ-Al_2O_3 catalysts with different Ni loadings (6 wt.%, 8 wt.%, and 10 wt.% Ni) are developed and investigated in the plasma-catalytic reforming of biogas in the RGA reactor. The properties of the catalysts are analyzed using a range of catalyst characterization techniques including surface area analyzer, inductivity coupled plasma (ICP), X-ray diffraction (XRD) and transmission electron microscopy (TEM) to better understand the effect of these catalysts on the plasma reforming reaction.

2. Experimental

2.1 Catalyst preparation and characterization

The catalysts used in this study are prepared by excess volume impregnation. Pelletized γ-Al_2O_3 with a particle size of 3 to 5 mm (Shanghai Jiuzhou Chemicals Co.) is used as support. The support is firstly impregnated with an aqueous solution of nickel nitrate and then stood overnight after sufficient agitation. The obtained samples are dried in air at 120 ℃ and then calcined at 400 ℃ for 6 h. Prior to plasma-catalytic biogas reforming reaction, the catalysts are reduced in a H_2 flow at 500 ℃ for 2 h.

The surface properties of the catalysts including pore size distribution and specific surface area are measured using a surface area analyzer (AUTOSORB-1-C, Quantachrome). The actual nickel loading of the catalysts is determined using an inductively coupled plasma instrument (ICP, iCAP6300, Thermo Scientific). The catalyst samples are extracted by concentrated nitric acid and hydrochloric acid for the ICP analysis. The XRD patterns of the catalysts are recorded by an X-ray diffractometer (Rigaku Ultima IV) equipped with Cu–Kα radiation (45 kV tube voltage and 40 mA tube current) in the scanning range 2θ between 10° and 80°. TEM (Tecnai G2 F20 S-TWIN)

147 analysis is used to examine the catalyst morphology and to estimate the size of Ni particles
148 dispersed over the catalytic surface. The average Ni particle size can be estimated by measuring the
149 size of at least 100 Ni particles.

150 **2.2 Experimental setup**

151 Fig. 1 shows a schematic diagram of the experimental setup for the plasma-catalytic
152 reforming of biogas. The RGA reactor consists of a conical inner electrode (anode) and a
153 grounded cylindrical outer electrode (cathode), both made of stainless steel. The narrowest gap
154 between the two electrodes (for arc ignition) is 2 mm. The feed gas is injected into the reactor
155 through a three tangential inlet structure, to generate a swirling flow. A more detailed
156 description of the RGA reactor can be found in our previous work [26].

157 A high voltage DC power source (380 V/10 kV WWL-SS) is connected to the RGA reactor to
158 generate plasma and a 40 kΩ resistance is used as a current limiter. During the experiments, the
159 output voltage of the power source is kept constant at 10 kV. A mixture of CH_4 and CO_2 with a
160 fixed CH_4/CO_2 molar ratio of 3:7 is used as reactants.

161 Gas products are analyzed by a gas chromatography (GC9790A, Fuli Analytical Instrument),
162 equipped with a thermal conductivity detector (TCD) and a flame ionization detector (FID). A
163 catalyst bed is placed in the downstream of the plasma arc, while the distance between the tip of
164 the inner electrode and the catalyst bed is kept at 1.5 cm. Thus, the catalyst bed can partly
165 interact with the rotating arc.

166

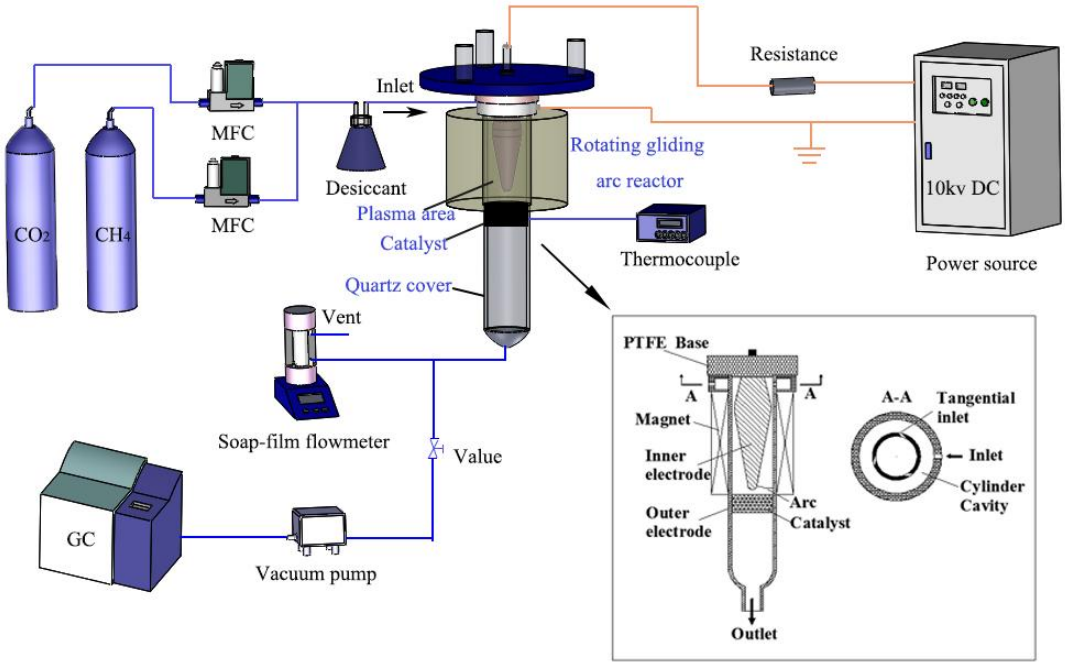

Fig. 1. Schematic diagram of RGA plasma-catalytic experimental setup

2.3 Parameter definition and calculation

The CH_4 conversion $X(CH_4)$ and CO_2 conversion $X(CO_2)$ are defined as follows:

$$X(CH_4)(\%)=\frac{\text{moles of } CH_4 \text{ converted}}{\text{moles of } CH_4 \text{ input}}\times 100\% \quad (1)$$

$$X(CO_2)(\%)=\frac{\text{moles of } CO_2 \text{ converted}}{\text{moles of } CO_2 \text{ input}}\times 100\% \quad (2)$$

The selectivity towards hydrogen $S(H_2)$, carbon monoxide $S(CO)$ and by-products $S(C_xH_y)$, and the yield of H_2 and CO can be calculated by:

$$S(H_2)(\%)=\frac{\text{moles of } H_2 \text{ produced}}{2\times\text{moles of } CH_4 \text{ converted}}\times 100\% \quad (3)$$

$$S(CO)(\%)=\frac{\text{moles of CO produced}}{\text{moles of } CH_4 \text{ converted}+\text{moles of } CO_2 \text{ converted}}\times 100\% \quad (4)$$

$$S(C_xH_y)(\%)=\frac{x\times\text{moles of } C_xH_y \text{ produced}}{\text{moles of } CH_4 \text{ converted}+\text{moles of } CO_2 \text{ converted}}\times 100\% \quad (5)$$

$$Y(H_2)(\%)=\frac{\text{moles of } H_2 \text{ produced}}{2\times\text{moles of } CH_4 \text{ input}}\times 100\% \quad (6)$$

$$Y(CO)(\%)=\frac{\text{moles of CO produced}}{\text{moles of } CH_4 \text{ input}+\text{moles of } CO_2 \text{ input}}\times 100\% \quad (7)$$

The H_2/CO molar ratio is defined as follows:

$$H_2/CO=\frac{\text{moles of } H_2 \text{ produced}}{\text{moles of CO produced}} \quad (8)$$

The specific energy consumption (SEC) for syngas production is calculated using the following equation:

$$SEC(kJ/mol)=\frac{\text{electricity consumption per unit time}}{\text{moles of } H_2 \text{ produced}+\text{moles of CO produced}}\times 100\% \quad (9)$$

3. Results and discussion

3.1 Catalyst characterization

Table 1 shows a fairly good agreement between the nominal and analyzed Ni content (by ICP), confirming the reliability of the method for the preparation of the catalysts. The weight of the catalyst sample used for each test is 50 mg.

Table 1. Ni content of the catalysts determined by ICP

Catalyst	Sample weight (mg)	Ni content (wt.%)
6 wt. % Ni/γ-Al_2O_3	50.8	6.16
8 wt. % Ni/γ-Al_2O_3	50.2	8.17
10 wt. % Ni/γ-Al_2O_3	50.6	10.00

The specific surface area of the catalysts is calculated by using the BET (Brunauer, Emmett and Teller) method, while the pore diameter distribution of the catalysts is determined from the adsorption isotherm. As shown in Fig. 2, the pore diameter distribution of the Ni catalysts is

196 significantly different to that of the catalyst support (γ-Al_2O_3), while the change of Ni loading has a
197 weak effect on the pore diameter distribution of the Ni/γ-Al_2O_3 catalysts. Table 2 presents the
198 specific surface area, pore volume, and average pore diameter of the Ni catalysts and support. These
199 results show that increasing Ni loading decreases the specific surface area and pore volume of the
200 catalysts. However, the average pore diameter of these Ni/γ-Al_2O_3 catalysts is larger than that of
201 γ-Al_2O_3 support. This difference might be attributed to the diffusing of Ni particles into smaller
202 pores of the γ-Al_2O_3 support during the catalyst preparation. [29].
203

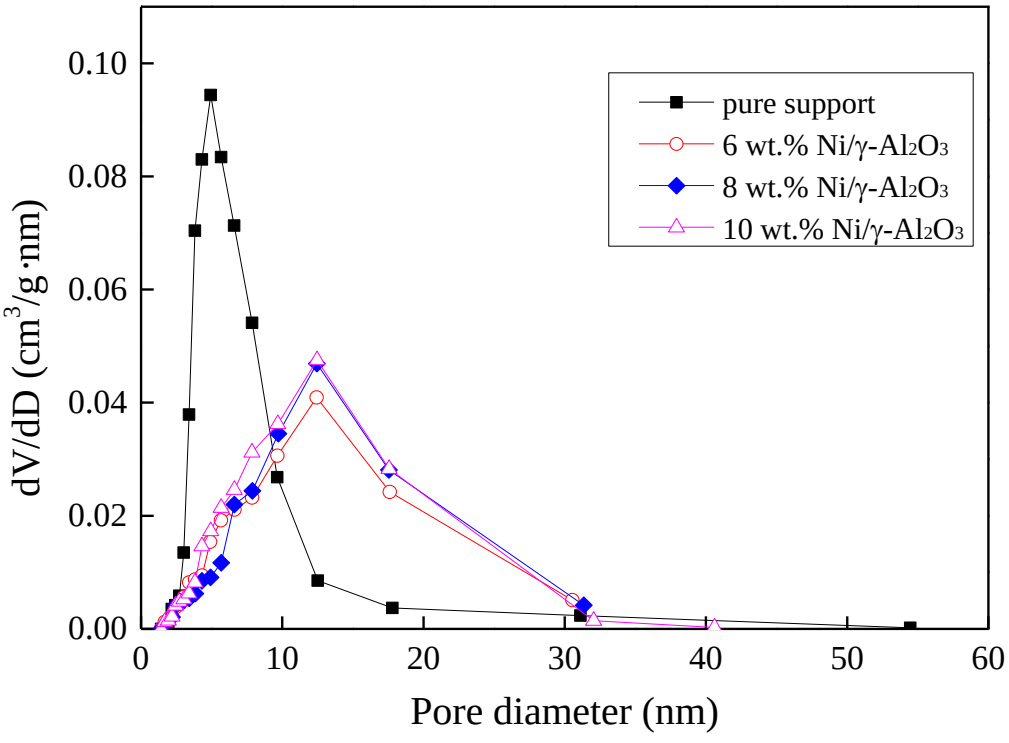

204
205 **Fig. 2.** Pore diameter distribution of the γ-Al_2O_3 support and Ni/γ-Al_2O_3 catalysts

206 Table 2. Physicochemical properties of the γ-Al_2O_3 support and Ni/γ-Al_2O_3 catalysts
207

Catalyst	Specific surface area (m^2/g)	Pore volume (cm^3/g)	Average pore diameter (nm)
γ-Al_2O_3	245.9	0.556	9.04
6 wt. %Ni/γ-Al_2O_3	176.5	0.488	11.07

8 wt. %Ni/γ-Al_2O_3	167.5	0.463	11.05
10 wt. %Ni/γ-Al_2O_3	148.3	0.438	11.80

Fig. 3 presents the XRD patterns of the reduced Ni/γ-Al_2O_3 catalysts. All the catalysts show similar diffraction patterns with a clear γ-Al_2O_3 structure at 2θ = 19.28°, 31.30°, 37.36°, 45.52°, 60.80° and 66.88°. The peaks of metallic Ni at 44.42°, 51.60° and 76.08° are also visible but with a slight different peak widths.

The average crystallite size of Ni particles can be determined using the Scherrer equation

$$d = \frac{0.89\lambda}{B\cos\theta} \times \frac{180°}{\pi} \quad (10)$$

where d is the mean Ni crystallite diameter, λ is the X-ray wavelength and B is the full width half maximum (FWHM) of the Ni peak. The average Ni particle size of the catalysts with different Ni loadings (6 wt. %, 8 wt. %, and 10 wt. %) is 10.5 nm, 10.1 nm, 9.6 nm, respectively. It is believed that the formation of smaller Ni particles on the catalyst could contribute to enhanced dispersion of Ni particles on the catalyst surface, and consequently enhance the activity of the catalyst, a statement supported by the results of plasma-catalytic biogas reforming in the following sections.

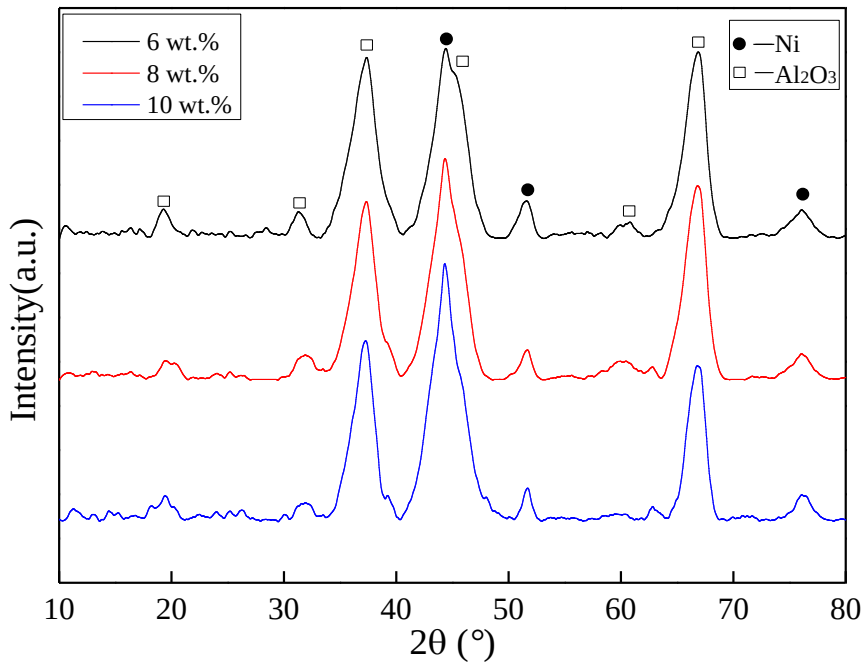

Fig. 3. XRD patterns of the reduced Ni/γ-Al_2O_3 catalysts before reaction

Fig. 4 shows the TEM images of the 10 wt. % Ni/γ-Al_2O_3 catalyst. Highly dispersed metallic Ni particles can be clearly observed. We find that the average Ni particle size of the 10 wt.% Ni/γ-Al_2O_3 catalyst is around 10 nm, which is in good agreement with the result determined using the Scherrer equation.

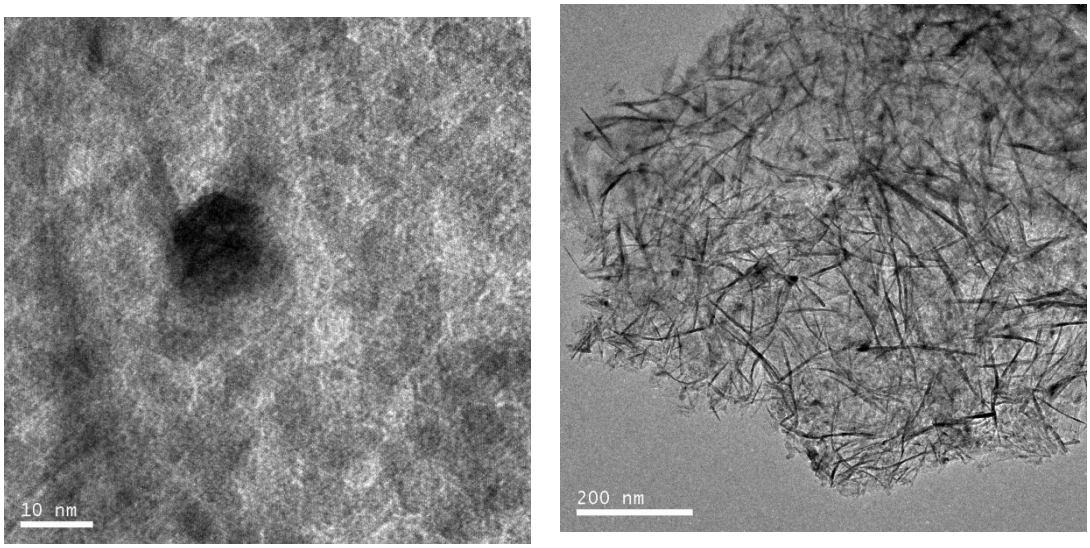

Fig. 4. TEM images of 10 wt.% Ni/γ-Al_2O_3 catalyst

3.2 Plasma biogas reforming without catalyst

Total feed flow rate is an important operating parameter: it is proportional to the processing capacity of the reactor and relates inversely to the retention time of the reactants in the plasma zone. Fig. 5 shows the effect of total feed flow rate on the performance of the plasma biogas reforming in the absence of a catalyst. Clearly, the conversion of CH_4 and CO_2 declines from 52.6% and 39.2% to 31.6% and 19.6%, respectively, when increasing the total feed flow from 6 to 20 L/min. It is found that the retention time of the reactants in the plasma zone, determined as the plasma volume (estimated by visual observation of the discharge zone) divided by total flow rate, significantly decreases from 101.8 to 30.5 ms when changing the total flow rate from 6 to 20 L/min, which reduces the chance of CO_2 and CH_4 reacting with energetic electrons and reactive species. On the other hand, increasing the total flow of CO_2 and CH_4 decreases the specific energy density of the plasma at a constant plasma power. The combined effects lead to the decreased conversion of CO_2 and CH_4 although the converted reactants increase when increasing the feed flow rate (Fig. 5a).

H_2 and CO are the major gas products in the plasma biogas reforming, while small amounts of C_2H_2 and C_2H_4 are also formed, as shown in Fig. 5b. The selectivity of these products declines slightly with rising total feed flow. In addition, the amount of C_2H_6 is almost negligible in the RGA reforming of biogas, with a selectivity of below 0.02%. Previous studies have shown that C_2H_6 is the dominant C_2 hydrocarbons in plasma biogas reforming using DBD reactors [14,30,31], while C_2H_2 and C_2H_4 are the dominant hydrocarbons in the plasma reforming of biogas using gliding arc discharges. Compared to DBD, gliding arc discharge has a significantly higher electron density which could change the reaction pathways (e.g. dehydrogenation of ethane) and consequently shift the distribution of C_2H_2, C_2H_4 and C_2H_6 in C_2 hydrocarbons. In the plasma biogas reforming

253 without a catalyst using a DBD, in addition to the production of syngas, a range of C_2-C_4
254 hydrocarbons are formed as by-products with low selectivity, which also decrease the energy
255 efficiency for syngas production. In this work, we find that the rotating gliding arc discharge could
256 generate much cleaner gas products of which syngas is the main one with limited amounts of C_2H_2
257 and C_2H_4. Similar results were also obtained in an AC flat gliding arc reactor [12,25,32].

258 Fig. 5c shows the yield of H_2 and CO and the variation of the H_2/CO molar ratio as a function of
259 total flow rate. The yield of H_2 and CO declines from 17.6% and 24.5% to 8.1% and 8.3%,
260 respectively, while the H_2/CO molar ratio slightly increases from 0.43 to 0.58 when the total flow
261 rate rises from 6 to 20 L/min. The results indicate that a lower total flow rate is beneficial for the
262 conversion of reactants and the production of more syngas. The H_2/CO molar ratio of the syngas
263 obtained is suitable for the further synthesis of long chain hydrocarbons through a Fischer-Tropsch
264 process. In addition, no obvious carbon deposition is observed in the plasma reaction at a CH_4/CO_2
265 molar ratio of 3:7

266

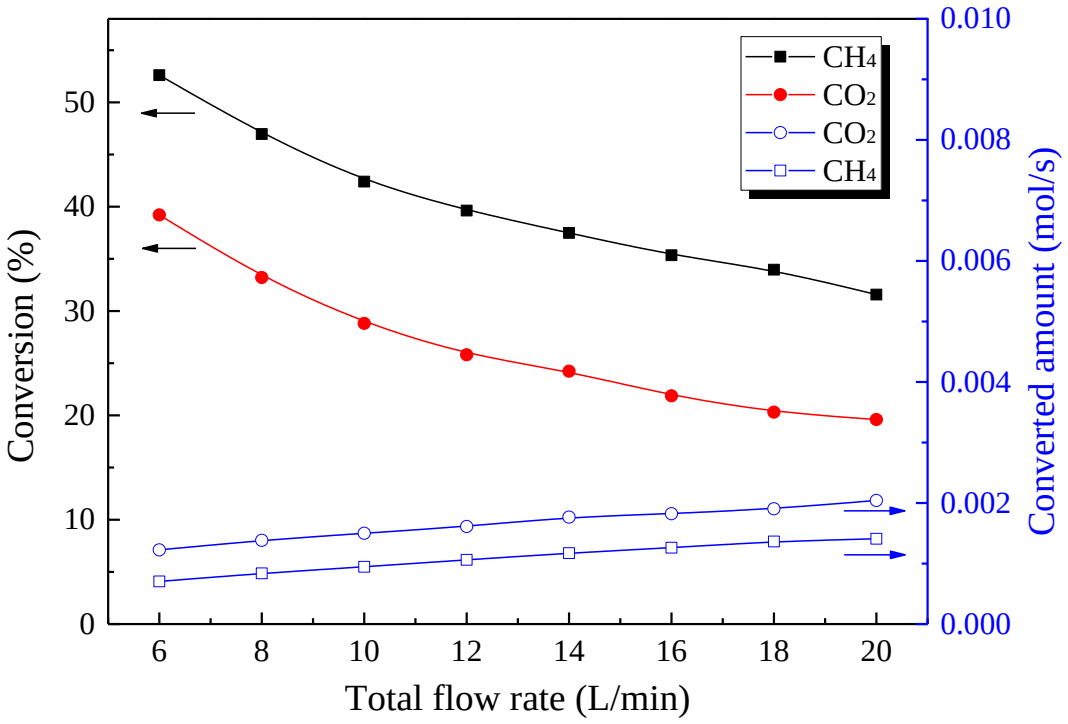
Conversion (%)
Converted amount (mol/s)
Total flow rate (L/min)
CH4
CO2
CO2
CH4
0
10
20
30
40
50
0.000
0.002
0.004
0.006
0.008
0.010
6
8
10
12
14
16
18
20

(a)

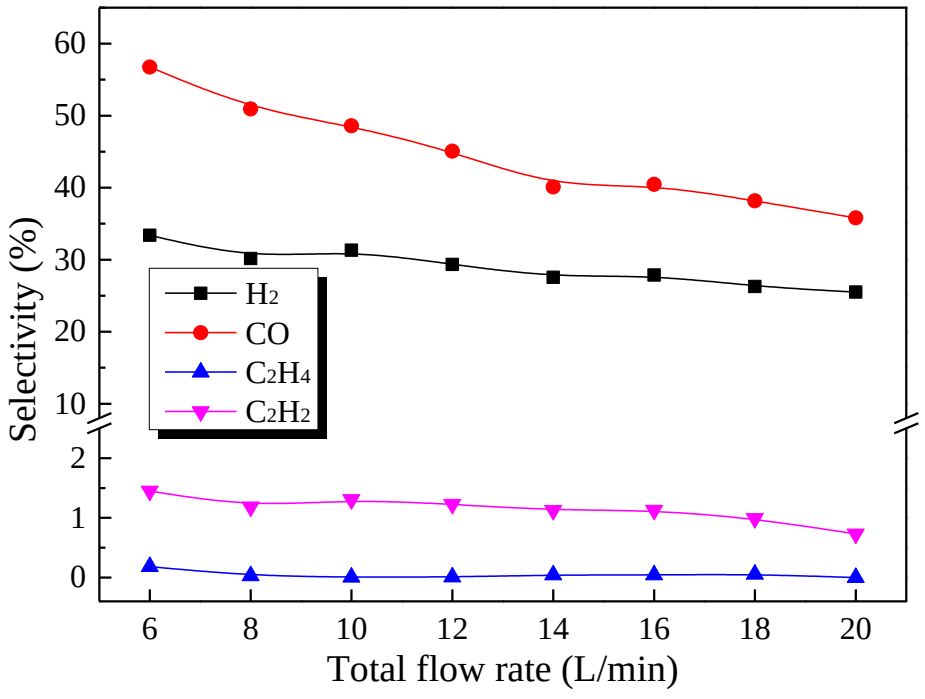
Selectivity (%)
Total flow rate (L/min)
H2
CO
C2H4
C2H2
0
1
2
10
20
30
40
50
60
6
8
10
12
14
16
18
20

(b)

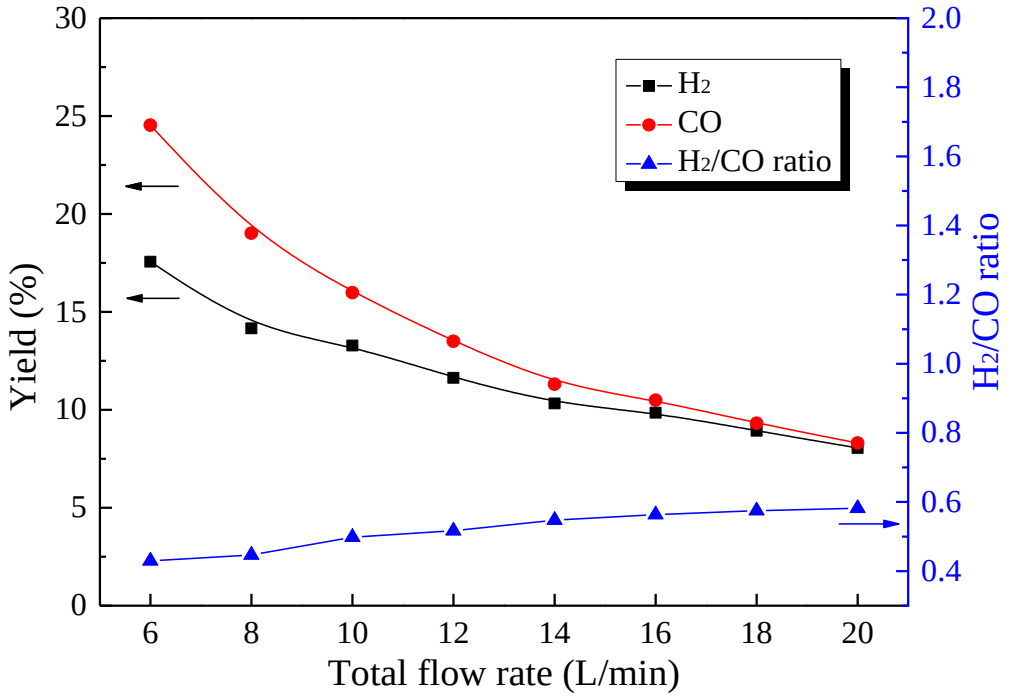

(c)

Fig. 5. Effect of total flow rate on (a) conversion and converted amount of CH_4 and CO_2, (b) selectivity of H_2, CO, C_2H_2 and C_2H_4, and (c) yield of H_2 and CO, and H_2/CO molar ratio

The reaction mechanism in the plasma reforming of biogas is very complex because of the formation of energetic electrons, excited molecules, radicals and ions, and the interactions of these species with reactants and their intermediates. Generally, electron-impact reactions account for most of the plasma-induced chemical reactions since electrons are far lighter than heavy particles [33]. CO_2 dissociation in non-thermal plasmas can be stimulated by the vibrational or electronic excitation of CO_2 molecules and dissociative attachment of electrons. It is well known that the vibrational excitation mechanism (Eq. (11-12)) is the most effective reaction route for CO_2 dissociation in non-thermal plasmas. At average electron energy of 1-2 eV, the electrons produced in plasma mostly provide excitation of low vibrational levels $CO_2^*(^1\Sigma^+)$. Then vibrational-vibrational (VV) relaxation processes lead to the population of highly excited vibrational states with

non-adiabatic transition $^1\Sigma^+ \rightarrow {}^3B_2$ and dissociation. When electron energies in plasma are high, the electronic excitation via Eq. (13) can be a dominant pathway for CO_2 dissociation, resulting in the formation of electronically excited CO. Note that - although the energy threshold of the dissociative attachment (Eq. (14)) is lower than that of dissociation through electronic excitation - the contribution of dissociative attachment is not significant, due to its low cross-section ($\approx 10^{-18}$ cm^2) [34,35].

$$CO_2^*(^1\Sigma^+) \rightarrow CO(^1\Sigma^+) + O(^1D) \quad (E_a \approx 7\ e \quad (11)$$

$$CO_2^*(^1\Sigma^+) \rightarrow CO_2^*(^3B_2) \rightarrow CO(^1\Sigma^+) + O(^3P) \quad (E_a = 5.5\ e \quad (12)$$

$$e + CO_2(^1\Sigma^+) \rightarrow CO(a^3\Pi) + O(^3P) + e \quad (E_a = 11.45 \quad (13)$$

$$e + CO_2 \rightarrow CO + O^- \quad (E_a = 4.4\ e \quad (14)$$

The dissociation of CH_4 is even more complicated than that of CO_2 in non-thermal plasmas, since methane molecule consists of five atoms and has more complex vibration modes. Based on the previous experimental and modeling studies on plasma dry reforming of methane, electron impact dissociation of CH_4 to produce CH_x (x=1-3) via Eq. (15-17) has been considered as the most important reactions for methane consumption [14,36,37]. In addition, the excited oxygen atoms $O(^1D)$ created in Eq. (11) are able to participate in a secondary reaction stepwise abstracting H from CH_4 molecules via Eq. (18) [38,39]. Here E_a is the electron threshold energy.

$$e + CH_4 \rightarrow CH_3 + H + e \quad (E_a = 9\ e \quad (15)$$

$$e + CH_4 \rightarrow CH_2 + H_2 + e \quad (E_a = 10\ e \quad (16)$$

$$e + CH_4 \rightarrow CH + H_2 + H + e \quad (E_a = 11\ e \quad (17)$$

$$O(^1D) + CH_4 \rightarrow CH_3 + OH \quad (18)$$

3.3 Plasma-catalytic reforming of biogas

To evaluate the effect of the Ni/γ-Al_2O_3 catalysts on the plasma reforming of biogas, the plasma reaction with pure γ-Al_2O_3 support and without a catalyst is also carried out for comparison. The total flow rate of the feed gas is fixed at 6 L/min and the corresponding gas hourly space velocity (GHSV) is 13000 h^{-1} in the plasma-catalytic biogas reforming.

Compared to the plasma biogas reforming without a catalyst, placing the γ-Al_2O_3 support in the downstream of the RGA reactor slightly increases the conversion of CH_4 and CO_2, but decreases the yield of H_2 and CO, as shown in Fig. 6. The coupling of the plasma with the Ni/γ-Al_2O_3 catalysts in the RGA reactor enhances the conversion of CH_4 compared to the biogas reforming in the absence of a catalyst. In addition, the conversion of CH_4 increases with the increase of the Ni loading and reaches the maximum of 58.5% using a 10 wt.% Ni/γ-Al_2O_3 catalyst, which could be attributed to the increased catalytic activity due to decreased Ni particle size and enhanced Ni dispersion on the catalyst surface at a higher Ni loading. Packing the Ni catalysts in the RGA reactor also increases the H_2 yield from 17.6% (without catalyst) to 20.7% due to enhanced CH_4 conversion. However, the presence of the Ni catalysts in the RGA reactor has a weak effect on the conversion of CO_2 conversion compared to the plasma-alone reaction. Similar results were also reported in previous studies using DBD or gliding arc [14] [40]. In this study, we find the effect of the Ni catalysts on the conversion of reactants is not significant, which might be ascribed to the partly interactions between the rotating arc and the catalyst as the catalyst bed is placed in the downstream of the plasma arc and might not be fully interacted with the plasma arc. In addition, the presence of the catalyst bed in the downstream of the rotating arc might also affect the propagation of the arc and plasma properties when the arc contacts with the catalyst bed, which in turn affects the plasma chemical

reactions.

Fig. 6c presents the influence of the catalysts on the SEC of the biogas reforming process. Compared to the reforming reaction using plasma-alone, the SEC of the plasma-catalytic reforming process is decreased when placing the Ni catalysts in the downstream of the RGA reactor. However, the presence of the γ-Al_2O_3 support in the reactor increases the SEC of the process compared to the reforming reaction using plasma-alone.

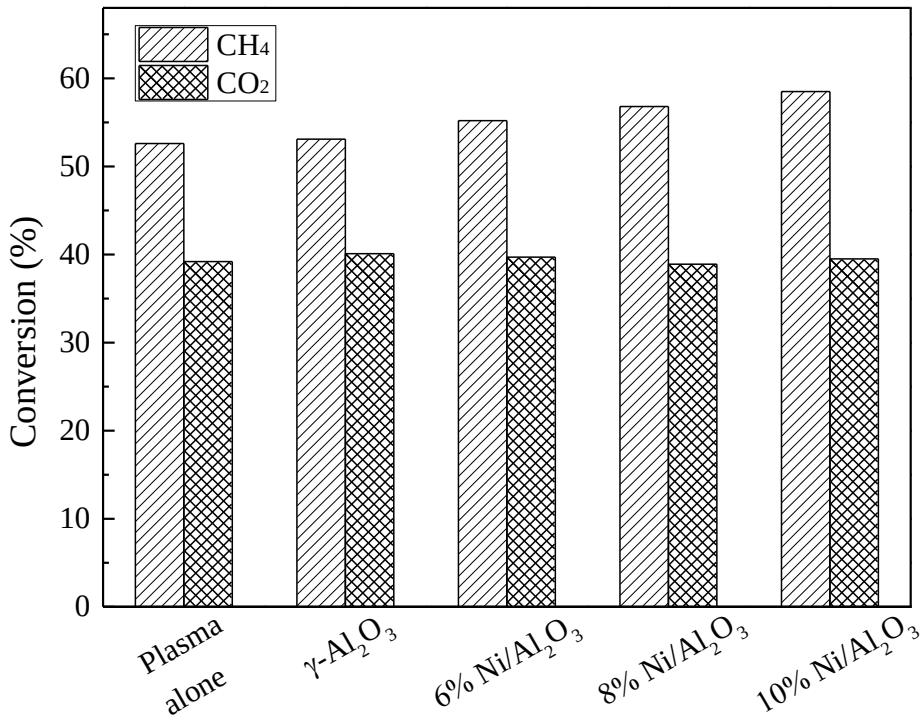

(a)

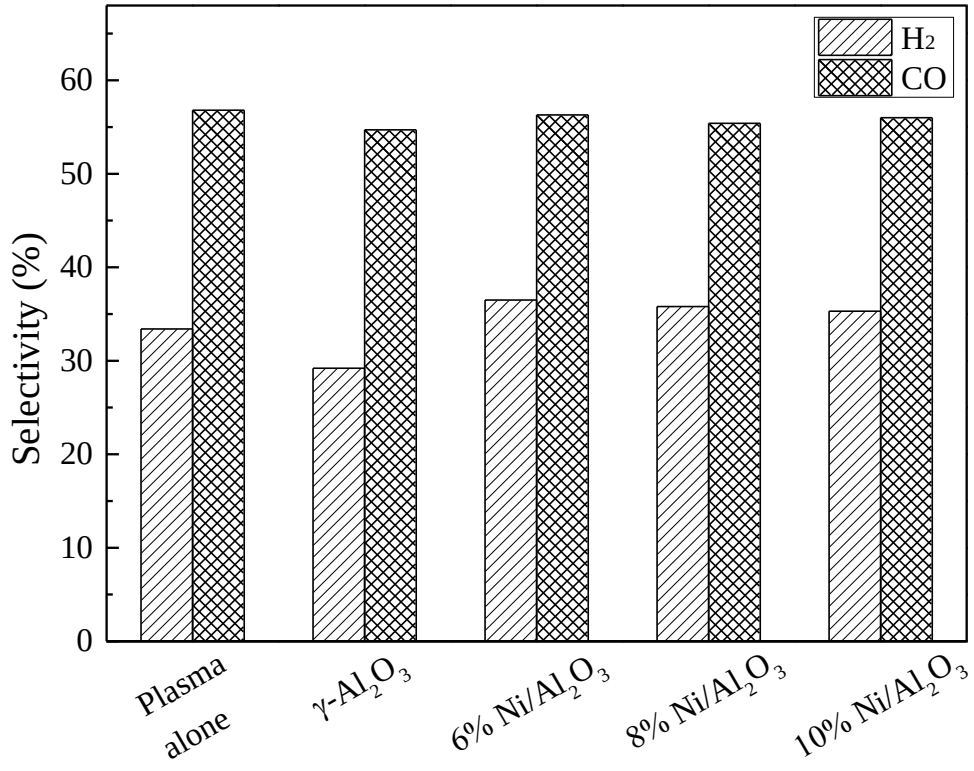

339

340 (b)

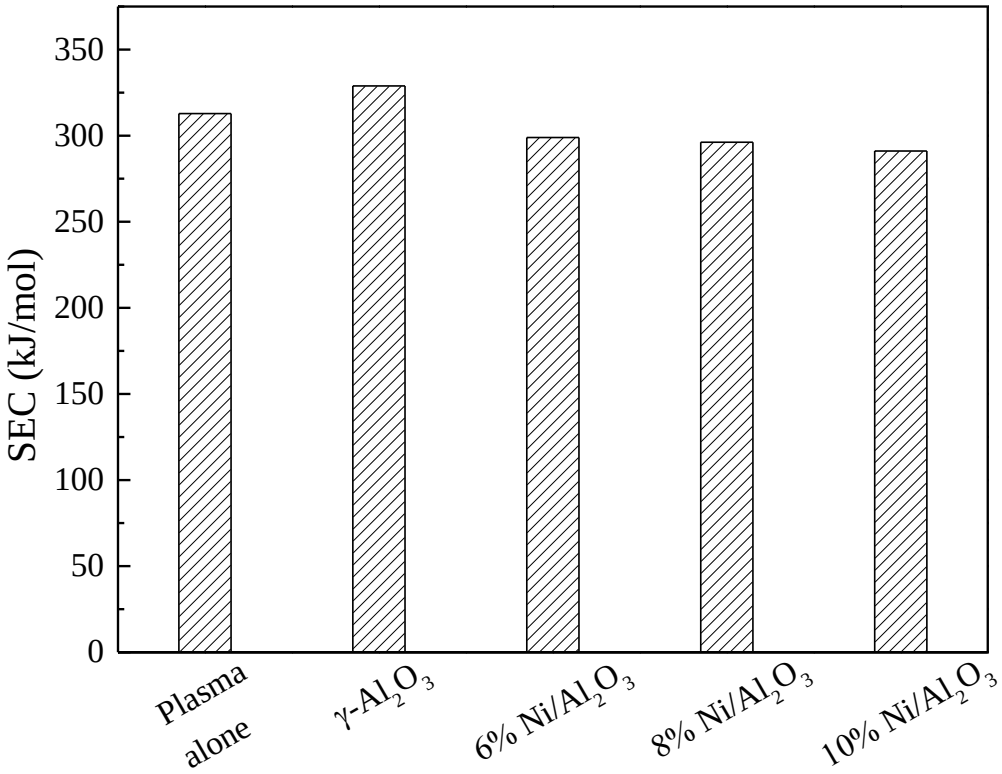

341

342 (c)

343 **Fig. 6.** Effect of catalysts on: (a) the conversion of CH_4 and CO_2, (b) the yield of H_2 and CO, and (c)

specific energy consumption

In the plasma-catalytic reforming of biogas, both gas phase reactions and surface reactions contribute to the dissociation and activation of CH_4 and CO_2, thus enhancing the conversion of biogas and syngas production [31,41]. There is a strong agreement in the literature that the mechanism of dry reforming of methane over a catalyst surface is bi-functional: CH_4 adsorption and dissociation mainly occurs on active metal surfaces, while CO_2 activation is promoted by the presence of surface defects [42]. In this study, CH_4 can be adsorbed and dissociated on the Ni particles formed over the catalyst surface. As shown in Fig. 6, increasing the Ni loading from 6% to 10% enhances the conversion of CH_4 and hydrogen yield. In addition, the average Ni particle size of the catalyst is decreased when increasing the Ni loading, which could enhance the dispersion of Ni particles on the catalyst surface. Both reduced Ni particle size and enhanced Ni dispersion lead to the enhanced catalytic activity. There is a clear relationship between the Ni loading and catalytic activity for CH_4 adsorption, dissociation and desorption. In the plasma-catalytic process, the generated intermediates on the catalyst surface might also interact with reactive species in the gas phase. It is generally accepted that CO_2 chemisorption and dissociation on a transition metal surface is dominated by electron transfer and requires the formation of an anionic CO_2^- precursor [43]. However, we find the influence of the Ni catalysts on the conversion of CO_2 is very weak in the plasma-catalytic reforming of biogas, which suggests that CO_2 adsorption and dissociation on the Ni surfaces and γ-Al_2O_3 support could be very limited. In addition, the yield of H_2 is lower than that of CO in the plasma reforming of biogas regardless the use of a catalyst (Fig. 6b), which might be attributed to the occurrence of reverse water gas shift reaction (Eq. (19)) as water droplets are

366 observed in the experiment. Moreover, no obvious carbon deposition is found, as the excess CO_2 in
367 the biogas provides an oxidizing atmosphere, which guarantees the activity and stability of the
368 catalyst to a large extent.

369 $$CO_2 + H_2 \rightarrow CO + H_2O \quad (19)$$

370 Table 3 shows a comparison of the performance of biogas reforming using different non-thermal
371 plasmas. We use the SEC as a key performance indicator in the comparison without considering the
372 cost of catalysts. Although high product selectivity could be achieved in biogas reforming using
373 corona and DBD plasmas, their SEC is at least one order of magnitude higher than the reforming
374 process using the RGA reactor in this work. In addition to the lowest SEC for biogas reforming, the
375 RGA system provides a relatively high conversion of CH_4 (58.5%) and CO_2 (39.5%), associated
376 with a moderate selectivity of H_2 (35.3%) and CO (56%). Moreover, the RGA reactor provides a
377 much larger processing capacity compared to traditional GA reactors with knife-shaped electrodes
378 as well as other non-thermal plasmas (e.g. DBD). Clearly, the RGA reactor combined with catalysts
379 has great potential for future industrial applications.
380

381 Table 3. Comparison of biogas reforming using different non-thermal plasmas
382

Plasma reactor	Catalyst	Flow rate (mL/min)	CH_4/CO_2 molar ratio	Power (W)	Conversion (%)		Selectivity (%)		SEC (kJ/mol)	Reference
					CH_4	CO_2	H_2	CO		
Corona	None	43	1:1	46.3	62.4	47.8	70	66.8	1798	[44]
Corona	Zeolites	25	1:1	8.4	56.3	22.8	-	9.1	4022	[45]
DBD	Ni/γ-Al_2O_3	30	1:1	38.4	44	26	~95	~95	2292	[46]
DBD	Ni/γ-Al_2O_3	50	1:1	50	38	21.2	27.6	45.3	5723	[14]

GA	None	150	7:3	-	21.5	5.7	57.1	14.9	1685	[3]
GA	None	1000	1:1	190	~40	~31	~62	~50	608	[47]
RGA	Ni/γ-Al_2O_3	6000	3:7	490	58.5	39.5	35.3	56	291.1	This work

Further improvement of the performance of the biogas reforming process can be expected by developing new reactor designs or innovative plasma-catalyst coupling approaches to enhance the interactions between the plasma and catalyst to further decrease the energy consumption of the plasma process, e.g. fluidised bed plasma-catalyst reactor or coating catalysts on the electrodes. Using pulsed power sources has great potential to further enhance the energy efficiency for the conversion and syngas production. Catalyst has been regarded as a key in plasma-catalytic chemical reactions. However, compared to thermal catalytic reforming of biogas, a very limited number of catalysts have been examined in plasma-catalytic reforming of biogas especially in the combination with a gliding arc discharge. The knowledge of selecting suitable catalysts for this reaction is very limited. Screening a range of catalysts that have been found effective in thermal catalytic reforming of biogas in the plasma-catalytic process is essential. Design and developing new, highly active and stable catalysts suitable for plasma-catalytic reforming of biogas is a key to push beyond the current state-of-the-art.

4. Conclusion

In this study, the rotating gliding arc plasma coupled with a downstream Ni/Al_2O_3 catalyst bed has been developed for the conversion of CO_2-rich biogas into syngas. The effect of the Ni/Al_2O_3 catalysts with different Ni loadings on the performance of the plasma biogas reforming process has

been investigated in terms of the conversion of reactant, selectivity and yield of syngas, as well as the energy efficiency of the process. In the plasma reforming without a catalyst, the highest CH_4 conversion of 52.6% is achieved at a CH_4/CO_2 molar ratio of 3:7 and a total flow rate of 6 L/min. The major products are H_2 and CO with small amount of C_2H_2 and C_2H_4. Compared to biogas reforming using other non-thermal plasmas (e.g. DBD), the RGA reforming process produces much cleaner gas products in which syngas is the major one. The flow rate of the reactants is found to significantly affect the conversion of CH_4 and CO_2 and the yield of syngas due to the change of retention time of the reactants in the plasma zone and specific energy density. Compared to the plasma reforming without using a catalyst, the coupling of the RGA with the Ni/Al_2O_3 catalysts placed in the downstream of the reactor enhances the performance of the reforming process. The results show that increasing the Ni loading from 6 wt% to 10 wt.% enhances the conversion of CH_4 and hydrogen yield, which can be attributed to the enhanced catalyst activity due to the reduced Ni particle size and enhanced dispersion of Ni particles on the catalyst surface when using a higher Ni loading amount. The maximum CH_4 conversion of 58.5% and H_2 yield of 20.7% are achieved when the 10 wt.% $Ni/\gamma\text{-}Al_2O_3$ catalyst is placed downstream of the RGA reactor. Compared to traditional knife-shaped gliding arc plasma or other non-thermal plasmas, the RGA reactor used in this work provides a relatively higher conversion of biogas and a much larger processing capacity with significantly enhanced energy efficiency of the process.

Acknowledgement

The support of this work by the National Nature Science Foundation of China (No. 51576174), UK EPSRC SUPERGEN Hydrogen & Fuel Cell (H2FC) Research Hub (EP/J016454/1, Ref

EACPR_PS5768) and the Royal Society (Newton Advanced Fellowship, Ref. NA140303) is gratefully acknowledged. We also acknowledge the financial support of the Program of Introducing Talents of Discipline to University (B08026) and the Pao Yu-Kong International Fund. Fengsen Zhu acknowledges the financial support of China Scholarship Council (CSC), Newton Fund and British Council (UK-China PhD Placement Grant).

References:

[1] Weiland P. Biogas production: current state and perspectives. Appl Microbiol Biot. 2010;85:849-60.

[2] Lau CS, Tsolakis A, Wyszynski ML. Biogas upgrade to syn-gas (H_2–CO) via dry and oxidative reforming. Int J Hydrogen Energy. 2011;36:397-404.

[3] Rueangjitt N, Akarawitoo C, Chavadej S. Production of Hydrogen-Rich Syngas from Biogas Reforming with Partial Oxidation Using a Multi-Stage AC Gliding Arc System. Plasma Chem Plasma P. 2012;32:583-96.

[4] Tao X, Bai M, Li X, Long H, Shang S, Yin Y, et al. CH4–CO_2 reforming by plasma – challenges and opportunities. Prog Energy Combust. 2011;37:113-24.

[5] Heintze M, Pietruszka B. Plasma catalytic conversion of methane into syngas: the combined effect of discharge activation and catalysis. Catal Today. 2004;89:21-25.

[6] Haryanto A, Fernando S, Murali N, Adhikari S. Current Status of Hydrogen Production Techniques by Steam Reforming of Ethanol: A Review. Energy Fuels. 2005;19:2098-106.

[7] Koo KY, Roh H, Seo YT, Seo DJ, Yoon WL, Park SB. Coke study on MgO-promoted Ni/Al_2O_3 catalyst in combined H_2O and CO_2 reforming of methane for gas to liquid (GTL) process. Appl Catal A: Gen. 2008;340:183-90.

[8] Roh H, Koo KY, Yoon WL. Combined reforming of methane over co-precipitated Ni–CeO_2, Ni–ZrO_2 and Ni–$Ce_{0.8}Zr_{0.2}O_2$ catalysts to produce synthesis gas for gas to liquid (GTL) process. Catal Today. 2009;146:71-75.

[9] Pietruszka B, Anklam K, Heintze M. Plasma-assisted partial oxidation of methane to synthesis gas in a dielectric barrier discharge. Appl Catal A: Gen. 2004;261:19-24.

[10] Jin R, Chen Y, Li W, Cui W, Ji Y, Yu C, et al. Mechanism for catalytic partial oxidation of methane to syngas over a Ni/Al_2O_3 catalyst. Appl Catal A: Gen. 2000;201:71-80.

[11] Wang Q, Cheng Y, Jin Y. Dry reforming of methane in an atmospheric pressure plasma fluidized bed with Ni/γ-Al_2O_3 catalyst. Catal Today. 2009;148:275-82.

[12] Bo Z, Yan J, Li X, Chi Y, Cen K. Plasma assisted dry methane reforming using gliding arc gas discharge: Effect of feed gases proportion. Int J Hydrogen Energy. 2008;33:5545-53.

[13] Wang Q, Yan B, Jin Y, Cheng Y. Investigation of Dry Reforming of Methane in a Dielectric Barrier Discharge Reactor. Plasma Chem Plasma P. 2009;29:217-28.

[14] Tu X, Whitehead JC. Plasma-catalytic dry reforming of methane in an atmospheric dielectric

462 barrier discharge: Understanding the synergistic effect at low temperature. Appl Catal B: Environ.
463 2012;125:439-48.
464 [15] Gallon HJ, Tu X, Whitehead JC. Effects of Reactor Packing Materials on H_2 Production by
465 CO_2 Reforming of CH_4 in a Dielectric Barrier Discharge. Plasma Processes Polym. 2012;9:90-97.
466 [16] Li M, Xu G, Tian Y, Chen L, Fu H. Carbon Dioxide Reforming of Methane Using DC Corona
467 Discharge Plasma Reaction. J Phys Chem A. 2004;108:1687-93.
468 [17] Ghorbanzadeh AM, Lotfalipour R, Rezaei S. Carbon dioxide reforming of methane at near
469 room temperature in low energy pulsed plasma. Int J Hydrogen Energy. 2009;34:293-98.
470 [18] Zhang J, Zhang J, Yang Y, Liu Q. Oxidative Coupling and Reforming of Methane with Carbon
471 Dioxide Using a Pulsed Microwave Plasma under Atmospheric Pressure. Energy Fuels.
472 2003;17:54-59.
473 [19] Chen HL, Lee HM, Chen SH, Chao Y, Chang MB. Review of plasma catalysis on hydrocarbon
474 reforming for hydrogen production—Interaction, integration, and prospects. Appl Catal B: Environ.
475 2008;85:1-09.
476 [20] Marques R, Da Costa S, Da Costa P. Plasma-assisted catalytic oxidation of methane: On the
477 influence of plasma energy deposition and feed composition. Applied Catalysis B: Environmental.
478 2008;82:50-57.
479 [21] Rueangjitt N, Sreethawong T, Chavadej S, Sekiguchi H. Plasma-catalytic reforming of methane
480 in AC microsized gliding arc discharge: Effects of input power, reactor thickness, and catalyst
481 existence. Chem Eng J. 2009;155:874-80.
482 [22] Zhang Y, Chu W, Cao W, Luo C, Wen X, Zhou K. A Plasma-Activated Ni/α-Al_2O_3 Catalyst
483 for the Conversion of CH_4 to Syngas. Plasma Chem Plasma P. 2000;20:137-44.
484 [23] Song HK, Choi J, Yue SH, Lee H, Na B. Synthesis gas production via dielectric barrier
485 discharge over Ni/γ-Al_2O_3 catalyst. Catal Today. 2004;89:27-33.
486 [24] Longa H, Shanga S, Taob X, Yinb Y, Dai X. CO_2 reforming of CH_4 by combination of cold
487 plasma jet and Ni/g-Al_2O_3 catalyst. Int J Hydrogen Energy. 2008;33:5510-15.
488 [25] Tu X, Whitehead JC. Plasma dry reforming of methane in an atmospheric pressure AC gliding
489 arc discharge: Co-generation of syngas and carbon nanomaterials. Int J Hydrogen Energy.
490 2014;39:9658-69.
491 [26] Zhang H, Du C, Wu A, Bo Z, Yan J, Li X. Rotating gliding arc assisted methane
492 decomposition in nitrogen for hydrogen production. Int J Hydrogen Energy. 2014;39:12620-35.
493 [27] Li XD, Zhang H, Yan SX, Yan JH, Du CM. Hydrogen production from partial oxidation of
494 methane using an AC rotating gliding arc reactor. Plasma Sci, IEEE Trans. 2013;41:126-32.
495 [28] Wu A, Yan J, Zhang H, Zhang M, Du C, Li X. Study of the dry methane reforming process
496 using a rotating gliding arc reactor. Int J Hydrogen Energy. 2014;39:17656-70.
497 [29] Shang S, Liu G, Chai X, Tao X, Li X, Bai M, et al. Research on Ni/γ-Al_2O_3 catalyst for CO_2
498 reforming of CH_4 prepared by atmospheric pressure glow discharge plasma jet. Catal Today.
499 2009;148:268-74.
500 [30] Zhang Y, Li Y, Wang Y, Liu C, Eliasson B. Plasma methane conversion in the presence of
501 carbon dioxide using dielectric-barrier discharges. Fuel Process Technol. 2003;83:101-09.
502 [31] Sentek J, Krawczyk K, Młotek M, Kalczewska M, Kroker T, Kolb T, et al. Plasma-catalytic
503 methane conversion with carbon dioxide in dielectric barrier discharges. Appl Catal B: Environ.
504 2010;94:19-26.
505 [32] Allah ZA, Whitehead JC. Plasma-catalytic dry reforming of methane in an atmospheric

pressure AC gliding arc discharge. Catal Today. 2015;256, Part 1:76-79.
[33]Chung W, Chang M. Review of catalysis and plasma performance on dry reforming of CH_4 and possible synergistic effects. Renew Sust Energy Rev. 2016;62:13-31.
[34]McConkey JW, Malone CP, Johnson PV, Winstead C, McKoy V, Kanik I. Electron impact dissociation of oxygen-containing molecules–A critical review. Phys Rep. 2008;466:1-103.
[35]Fridman A. Plasma chemistry: Cambridge university press; 2008.
[36]Yang Y. Direct Non-oxidative Methane Conversion by Non-thermal Plasma: Modeling Study. Plasma Chem Plasma P. 2003;23:327-46.
[37]Kado S, Urasaki K, Sekine Y, Fujimoto K, Nozaki T, Okazaki K. Reaction mechanism of methane activation using non-equilibrium pulsed discharge at room temperature. Fuel. 2003;82:2291-97.
[38]Oumghar A, Legrand JC, Diamy AM, Turillon N. Methane conversion by an air microwave plasma. Plasma Chem Plasma P. 1995;15:87-107.
[39]Zhou LM, Xue B, Kogelschatz U, Eliasson B. Partial Oxidation of Methane to Methanol with Oxygen or Air in a Nonequilibrium Discharge Plasma. Plasma Chem Plasma P. 1998;18:375-93.
[40]Zeng Y, Zhu X, Mei D, Ashford B, Tu X. Plasma-catalytic dry reforming of methane over γ-Al_2O_3 supported metal catalysts. Catal Today. 2015;256, Part 1:80-87.
[41]Istadi, Amin NAS. Co-generation of synthesis gas and C2+ hydrocarbons from methane and carbon dioxide in a hybrid catalytic-plasma reactor: A review. Fuel. 2006;85:577-92.
[42]Pakhare D, Spivey J. A review of dry (CO_2) reforming of methane over noble metal catalysts. Chem Soc Rev. 2014;43:7813-37.
[43]Bradford M.C.J, Vannice M.A. CO_2 Reforming of CH_4. Catal Rev. 1999;41:1-42.
[44]Yang Y. Methane Conversion and Reforming by Nonthermal Plasma on Pins. Ind Eng Chem Res. 2002;41:5918-26.
[45]Liu C, Mallinson R, Lobban L. Comparative investigations on plasma catalytic methane conversion to higher hydrocarbons over zeolites. Appl Catal A: Gen. 1999;178:17-27.
[46]Wang Q, Yan B, Jin Y, Cheng Y. Dry reforming of methane in a dielectric barrier discharge reactor with Ni/Al_2O_3 catalyst: interaction of catalyst and plasma. Energy Fuels. 2009;23:4196-201.
[47]Indarto A, Choi J, Lee H, Song HK. Effect of additive gases on methane conversion using gliding arc discharge. Energy. 2006;31:2986-95.